Design and Function of a Dendrimer-Based Therapeutic Nanodevice Targeted to Tumor Cells Through the Folate Receptor

Antonio Quintana,[1,2] Ewa Raczka,[1,2] Lars Piehler,[1] Inhan Lee,[1] Andrzej Myc,[1] Istvan Majoros,[1] Anil K. Patri,[1] Thommey Thomas,[1] James Mulé,[1] and James R. Baker, Jr.[1,3]

Received May 6, 2002; accepted May 31, 2002

Purpose. We sought to develop nanoscale drug delivery materials that would allow targeted intracellular delivery while having an imaging capability for tracking uptake of the material. A complex nanodevice was designed and synthesized that targets tumor cells through the folate receptor.

Methods. The device is based on an ethylenediamine core polyamidoamine dendrimer of generation 5. Folic acid, fluorescein, and methotrexate were covalently attached to the surface to provide targeting, imaging, and intracellular drug delivery capabilities. Molecular modeling determined the optimal dendrimer surface modification for the function of the device and suggested a surface modification that improved targeting.

Results. Three nanodevices were synthesized. Experimental targeting data in KB cells confirmed the modeling predictions of specific and highly selective binding. Targeted delivery improved the cytotoxic response of the cells to methotrexate 100-fold over free drug.

Conclusions. These results demonstrate the ability to design and produce polymer-based nanodevices for the intracellular targeting of drugs, imaging agents, and other materials.

KEY WORDS: dendrimer; nanotechnology; chemotherapeutic molecular modeling; methotrexate.

INTRODUCTION

Folic acid (FA) is internalized into cells through a high affinity, receptor-mediated process (1). FA-conjugated proteins, such as RNase, BSA, IgG, and ferritin are also taken into cells through the folate-receptor pathway in a nondestructive manner (2,3). Because the high affinity FA receptor is overexpressed in several human cancer cells (4,5,6), relative tumor selective targeting has been achieved with FA-conjugated antineoplastic drugs (7), antisense oligonucleotides (8), protein toxins (9), and imaging agents (10). However, the direct conjugation of folate to the bioactive molecule can lead to loss of targeting or alter the function of the conjugate, and most of the conjugates cannot be further modified to improve targeting or anti-tumor activity (2–10).

Polyamidoamine (PAMAM) dendrimers are highly branched macromolecules with well-defined architecture (11) that can serve as a unique platform for a variety of therapeutic and imaging agents (12–17). We have developed dendrimer-based nanodevices optimized to target complex therapeutics. This involved computer modeling of the nanodevices in the hydrated state to find modifications of the primary amine groups that would optimize targeting. From the modeling studies, we synthesized modified polymers and evaluated their uptake and internalization in tumor cells that overexpress the high affinity folate receptor. The behavior of these dendrimer nanodevices was in accordance with the modeling predictions indicating the potential for these devices to be computer designed.

MATERIALS AND METHODS

Materials and Reagents

FA, acetic acid, dimethylsulfoxide (DMSO), penicillin/streptomycin, fetal bovine calf serum (FBS), and bovine serum albumin (BSA) were purchased from Sigma (St. Louis, MO, USA). Trypsin-EDTA, Dulbecco's phosphate buffered saline (PBS), and RPMI 1640 medium (with or without FA) were obtained from Gibco/BRL (Gaithersburg, MD, USA).

Synthesis Procedures and Analysis

Folate/Fluorescein Dendrimer

Generation 5 PAMAM dendrimer was prepared and analyzed as described previously (18). Dendrimer (50 mg, 1.70 μmol) was dissolved in DMSO (2 mL) and sodium phosphate buffer (0.1 M, pH 9, 5 mL) under nitrogen for conjugation to fluorescein isothiocyanate (17.3 mg, 44 μmol, 0.2 equivalents per dendrimer primary amine). The mixture was stirred in the dark for approximately 24 h, then washed and ultrafiltered in Centricon tubes (10,000 MWCO; Amicon). Folate was conjugated to the dendrimer through an EDC linkage as described (15).

Acetamide and 2,3-Hydroxypropyl Capping of Dendrimers

A solution of the dendrimer (1.70 μmol) in 8 mL of 1:1 DMSO:0.1 M sodium phosphate buffer (pH 9) was prepared. The following was repeated four times: acetic anhydride (79 μL, 833 μmol per day) was added dropwise, stirred for several hours; the pH of the solution was adjusted back to nine, and then stirred overnight in the dark under nitrogen. On the fifth day, the small amount of white precipitate was removed by filtration through Celite. The orange filtrate was purified by exhaustive dialysis against deionized water, using a 10,000 MWCO membrane (Spectrum Medical Industries). The retentate was concentrated by rotary evaporation to produce 50.8 mg of orange solid. 2, 3-Hydroxypropyl was prepared in the same manner but with the addition of glycidol (110 μL per day) in place of acetic anhydride.

Carboxyl and Fluorescein-Carboxyl Capped Dendrimer

To a solution of succinic anhydride (18 mg; 179 μmol) in dry DMSO, dendrimer (50 mg; 1.2 μmol) in DMSO was

[1] Center for Biologic Nanotechnology, Department of Internal Medicine, University of Michigan Medical School, Ann Arbor, Michigan 48109-0648.

[2] Current Address: Department of Pharmacology, Faculty of Medicine and Odontology, University of the Basque Country, 48940 Leioa (Vizcaya), Spain.

[3] To whom correspondence should be addressed. (e-mail: jbakerjr@umich.edu)

0724-8741/02/0900-1310/0 © 2002 Plenum Publishing Corporation

added dropwise, then stirred at ambient temperature under an atmosphere of nitrogen in dark for 18h. The reaction mixture was diluted with water and dialyzed in deionized water using a 1000 MWCO regenerated cellulose dialysis membrane. The retentate was then concentrated *in vacuo* and lyophilized to give the acid-capped dendrimer conjugate. Analysis of the 1H NMR spectrum integration showed that there was an average of 16 fluorescein and 2.5 folate moieties per dendrimer conjugate.

Methotrexate Conjugation with an Amide or Ester Bond

In 3 mL of DMF and 1 mL of DMSO solvent mixture, 0.5 mg methotrexate (9.9×10^{-7}mol) and 2.6 mg of 1-[3-(Dimethylamino) propyl-3-ethylcarbodiimide hydrochloride (1.4×10^{-5} mol) were added. The mixture was allowed to react for 1 h at room temperature under nitrogen, with vigorous stirring. The methotrexate active ester was added dropwise into the 3.4 mg (9.9×10^{-8} mol) bifunctional dendrimer [G5-Ac(96)-FITC(5)-FA(3)] in 12 mL DI water. The reaction mixture was stirred at room temperature for 3 days and the G5-Ac_{96}-$FITC_5$-FA_3-MTX_4 formed was dialyzed and lyophilized. The ester linkage was developed similarly by adding methotrexate active ester to 5.5 mg (1.6×10^{-7}mol) of bifunctional dendrimer with hydroxyl surface

Theoretical Modeling of Conjugated Dendrimer Devices

Model building and molecular dynamics simulations were performed on an Onyx workstation (Silicon Graphics, Inc.; Mountain View, CA, USA) using the Insight II software package (Molecular Simulations Inc.; San Diego, CA, USA). A generation 5 PAMAM dendrimer (EDA core) was first built and simulated with the consistent valence force field (CVFF) (10) for 50 ps at 295 °K, after standard minimization and annealing processes. The primary amines of a PAMAM dendrimer were all protonated to simulate pH 7 conditions. A distance-dependent dielectric constant was used to shield electrical charges. Models of different configurations were simulated for 100 ps at 310 °K after minimization and annealing. To ensure equilibrated states, the conformations were collected after the simulations had reached at least 50 ps.

Biological Evaluation of Device Function

Experimental Procedures

The KB cell line is a human epidermoid carcinoma that overexpresses folate receptors, especially when grown in low folic acid medium (13). KB cells were purchased from the American Type Tissue Collection (ATCC; Manassas, VA, USA) and grown continuously as a monolayer at 37°C, and 5% CO_2 in FA deficient RPMI 1640 medium. This medium was supplemented with penicillin (100 units/mL), streptomycin (100 μg/mL), and 10% heat-inactivated FBS, yielding a final FA concentration approximately that of normal human serum. About 2×10^5 cells per well were seeded in 12-well plates the day before the experiments. An hour before initiating an experiment, the cells were washed four times with FA deficient RPMI 1640 medium, then 1 mL of FA deficient medium was put in each well. The cells were then incubated with the folate conjugates under these conditions except for the competitive antagonism by free FA experiments when free FA was added in specific concentrations to the media. After gentle mixing, the cultures were maintained at 37°C, and the cells were incubated with the folate conjugates for 30 min. For the 0°C experiments, the plates were put on ice 10 min before the addition of the conjugates, and the cells were maintained at this temperature during the entire experiment. At the end of the incubation period for all experiments, the medium was aspirated, and three consecutive washes with 2 mL ice-cold PBS were performed. The cells were harvested by scraping in 0.5 mL 0.1% BSA in PBS. Results were examined by flow cytometry using a FACS calibur flow cytometer (Becton Dickinson), and surface and interior localization of the conjugates was determined using a Bio-Rad MRC 600 confocal microscope (Bio-Rad Laboratories; Hercules, CA, USA) coupled to a Nikon Diaphot-TMD inverted microscope.

Analysis and Expression of the Results

The double reciprocal plot of the increase in cell fluorescence against the concentration of the conjugate was used to calculate the apparent affinities of the dendrimer-folate conjugates for the folate receptor. The results are expressed as mean values with the corresponding SD.

RESULTS

Modeling of Nanodevices

The conformational structure of the generation 5 PAMAM, fluorescein, folic acid nanodevice (G5-FITC-FA) was modeled using Molecular Dynamics simulations to test the effect of the different capping groups (Fig. 1). Local branch aggregation is observed (Fig. 1a), indicating possible intermolecular branch interaction. Local branch aggregation is still observed when the primary surface amine groups were capped with carboxy groups (Fig. 1c). Both of these molecules internalized the FA groups in our modeling suggesting a decreased potential for receptor interaction. Modeling showed that capping the surface amines with either 2,3-dihydroxypropyl or acetamide groups (yielding neutral surfaces) produced an overall relaxation of the molecular structure (Fig, 1b and 1d, respectively) due to the absence of repulsive forces from charged amines. The model of the 2,3-dihydroxypropyl-G5-FITC-FA demonstrated greater surface crowding than the other structures, because the number of hydroxyl groups is twice that of the acetamide or amine groups. Some of the FA moieties in this nanodevice also seem to be buried inside the dendrimer suggesting a reduced likelihood of receptor interaction. All of the FA moities in the acetamide derivative appeared to extend away from the surface of the dendrimer, optimizing the likelihood of receptor interaction.

We measured two radial distances of the FA from the center of mass of the nanodevice: to the FA-dendrimer linking point and to the center of the pteridinyl ring of a given folate group (Table I). The mean FA distance of the amine surfaced G5-FITC-FA is smaller than its radius of gyration, indicating internalization of the FA and poor accessibility to the receptor. The mean radius of gyration and mean FA distance are very similar in the carboxy-G5-FITC-FA, which increases the accessibility of FA to the receptors. One of the three FAs is far outside of the radius of gyration imply-

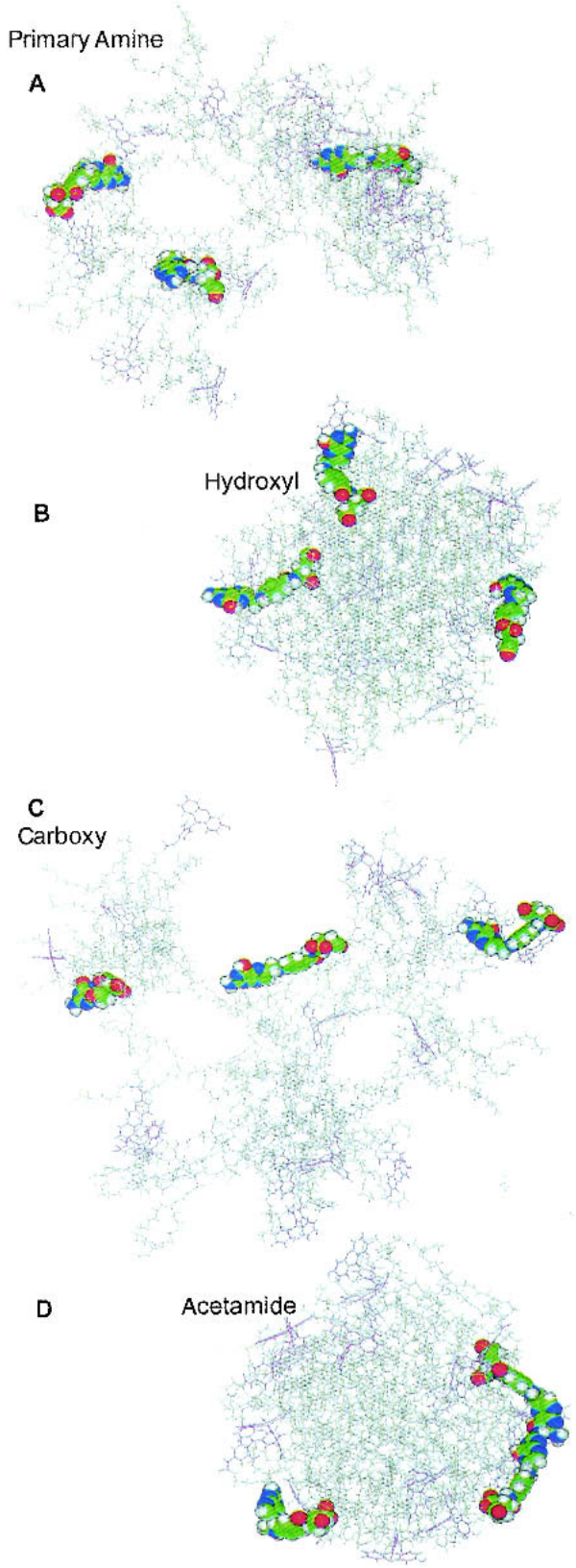

Fig. 1. Configuration of PAMAM G5 dendrimer-FITC-FA conjugates after 100 ps molecular dynamics simulation. The underlying G5 PAMAM dendritic structure is in grey; the FITC molecules are represented in pink; and the folic acid is space filled.

ing good potential access to FA receptors. The 2,3-dihydroxypropyl-G5-FITC-FA and acetamide-G5-FITC-FA nanodevices both show greater mean FA distances than the radius of gyration of the molecule. A significant portion of two of the three conjugated FA molecules are partially internalized in the 2,3-dihydroxypropyl-G5-FITC-FA suggesting potentially reduced accessibility of the whole FA molecule. In contrast, only one of three FA moieties in the acetamide-G5-FITC-FA is partially internalized in the dendrimer, with the other two FA molecules distributed on the surface.

Evaluation of the Biologic Function of the Dendrimer-Folate Nanodevices

Nontargeted Binding of Amine-Surfaced Nanodevices

G5-FITC-FA nanodevices bound poorly to KB cells showing minimal uptake at a 30 nM concentration only after long incubation times (4 h or greater). Control G5-FITC, lacking FA, gave similar uptake suggesting that the binding of both dendrimers was not the result of specific binding to the folate receptors. The presence of a high concentration (1μM) of free FA in the medium failed to block binding of the G5-FITC-FA also suggesting nontargeted binding to the cells.

Targeted Uptake of Dendrimers with Modified Surfaces

The binding of carboxy-G5-FITC-FA, 2,3-dihydroxypropyl-G5-FITC-FA, and acetamide-G5-FITC-FA nanodevices to KB cells was efficient and rapid occurring at a device threshold concentration of 10 nM after only 30 m at 37°C (Fig. 2a and 2b). Under these conditions, control nanodevices with identical surface modifications but without folate did not bind to KB cells. While all surface modifications with folate appeared capable of specifically targeting the cells, marked differences were apparent between the three surfaces in their respective ability to bind to KB cells (Fig. 2a and 2c). The apparent affinity and efficiency of internalization of the carboxyl nanodevice was markedly lower than that of the hydroxyl and acetamide nanodevices. A maximum increase in cell fluorescence (approximately 4 times baseline) was observed after the cells were incubated with 30 nM of carboxyl surfaced nanodevice and actually decreased when the cells were incubated in higher concentrations. The highest apparent affinity of any complex was observed with the acetamide-surfaced nanodevice requiring a concentration of only 23 nM to achieve 50% of maximal binding (Fig. 2c). The binding capacity was also high, allowing for a 20-fold increase in cell fluorescence after incubation with 300 nM for 30 min (Fig. 2b). The hydroxyl-surfaced nanodevice showed approximately half the affinity of the acetamide nanodevice (about 53 nM to achieve 50% of maximal binding), but displayed an overall binding capacity similar to the acetamide-surfaced device. We also performed experiments at 0°C to investigate ATP-dependent internalization through the high-affinity folate receptor, which is inactive at this temperature. The results (Fig. 2d) were qualitatively similar to those obtained at 37°C (Fig. 2c), but with lower overall increases in cell fluorescence.

The binding seen in the flow cytometry studies was confirmed in confocal microscopic images of the cells (Fig. 3a and 3b). The confocal analysis found uptake of the acetamide and

Table I. The Average Values of the Radial Distance of Folic Acid in G5-FITC-Folic Acid Conjugates with Different Surface Groups, as Found by Modeling

Surface group	Mean R_G (Å)[a]	Mean[a] folic acid distance[b] (Å)	Individual folic acid distances[c] (Å)	
			Dendrimer attached point	Center of the pteridinyl ring
Amine	29.5 ± 0.2	22.9 ± 5.3	27.2 ± 1.1	23.4 ± 1.3
			37.8 ± 0.8	29.0 ± 1.7
			24.6 ± 0.6	16.5 ± 1.4
Carboxyl	34.3 ± 0.2	34.9 ± 4.8	32.4 ± 0.9	30.7 ± 1.6
			34.2 ± 1.4	33.1 ± 1.6
			46.8 ± 1.5	41.0 ± 2.2
Hydroxyl	21.8 ± 0.1	27.2 ± 2.4	20.6 ± 0.6	30.2 ± 1.1
			17.0 ± 0.4	26.9 ± 0.3
			25.3 ± 0.5	24.6 ± 0.4
Acetamide	19.8 ± 0.1	26.7 ± 2.8	25.8 ± 1.1	23.4 ± 0.4
			18.7 ± 0.8	26.7 ± 0.5
			22.3 ± 0.6	30.0 ± 0.7

[a] Mean values are calculated from simulation time between 50 ps and 100 ps. R_G = radius of gyration.
[b] Mean folic acid distances are calculated from the center of mass to the center of the pteridinyl ring of folic acid groups.
[c] Radial distances are calculated from the center of mass.

hydroxyl nanodevices in the KB cells, but no uptake in NIH 3T3 cells, which lack a FA receptor. The acetamide capped G5-FI-FA material appeared to internalize over a period of 24 h (Fig. 3c). No concentration-dependent increases in uptake were noted with the carboxyl-surfaced molecule (data not shown). Control dendrimers with the various surface modifications (but without FA) also failed to bind to the cells (Fig 3d).

Competitive Inhibition of Nanodevice Binding and Internalization by Free FA

Increases in cell fluorescence from the uptake of the three surface-modified nanodevices were entirely blocked by the simultaneous presence of free FA in the medium. A free FA concentration of 25–30 nM reduced the cell fluorescence from either the acetamide or the hydroxyl nanodevices (at 30 nM) by 50%, suggesting the two had approximately similar affinity for the folate receptor. Only 40–50% of the three surface-modified nanodevices could be removed from the surface of cells after three acidic washes (pH 3) applied at the end of a 30 min incubation period at 0°C. This is in contrast to free folate, which is completely removed by this technique in concordance with prior reports.

Intracellular Drug Delivery Using Nanodevices

To evaluate intracellular deliver drug by the nanodevice, trifunctional devices were designed and synthesized. These devices had three chemically coupled molecules; a reporting fluorchrome (FITC), a targeting agent (folic acid), and a chemotherapeutic (methotrexate) conjugated either through a nonbiodegradable amide linkage or through an ester linkage that will hydrolyze at the low pH in the endosome releasing the methotrexate. Both types of methotrexate triple conjugate were internalized into KB cells *in vitro* as efficiently as folic acid targeted nanodevices not coupled to drug (Fig. 4a). Only the nanodevice that was designed to release drug after folate receptor mediated entry into the cell was cytotoxic, either acutely or in assays of surviving cell clones (Fig. 4b). Equimolar concentrations of free methotrexate were 4-fold less effective in killing the tumor cells than drug conjugated through ester linkages, while the conjugates with the amide linkage, and conjugates without drug, were not toxic at any concentration tested. This suggested improved cytotoxic efficiency due to intracellular drug delivery and release.

DISCUSSION

The delivery of biologically active materials to specific cells is an important and challenging goal. Current attempts at achieving delivery have revolved around the use of synthetic (microsphere) carrier molecules, which are too large to have access to cells or efficient uptake by cells. Most nanoscale materials currently used for carrier applications are biologically derived (e.g., proteins) leading to immunogenicity, are polydispersed in size or are inconsistent in structural characteristics (polylysine). Dendrimers are one of the first biocompatible, synthetic, nanoscaled materials that can be made with consistent structural characteristics producing a uniform population of molecules with predictable size and surface characteristics. These molecules are nonimmunogenic. They span the size range of proteins—a 1–10 nm diameter and a 1000 to 800,000 kDa molecular weight. Dendrimers are uniquely suited as carrier structures for drug or bioactive molecule delivery.

The development of complex nanodevices as delivery platforms for biomaterials is deceptively complicated and requires significant modification of the polymer carrier. Coupling reactions for targeting, signaling, or therapeutic moieties must be compatible with the previously coupled moieties. Interactions of the polymer backbone with these groups can alter their function. Merely the coexpression of several molecules of a given moiety on the polymer surface may lead to undesirable effects. Aggregation of nanostructures can result from interactions between different substituted groups and can inactivate or even precipitate the devices. The devel-

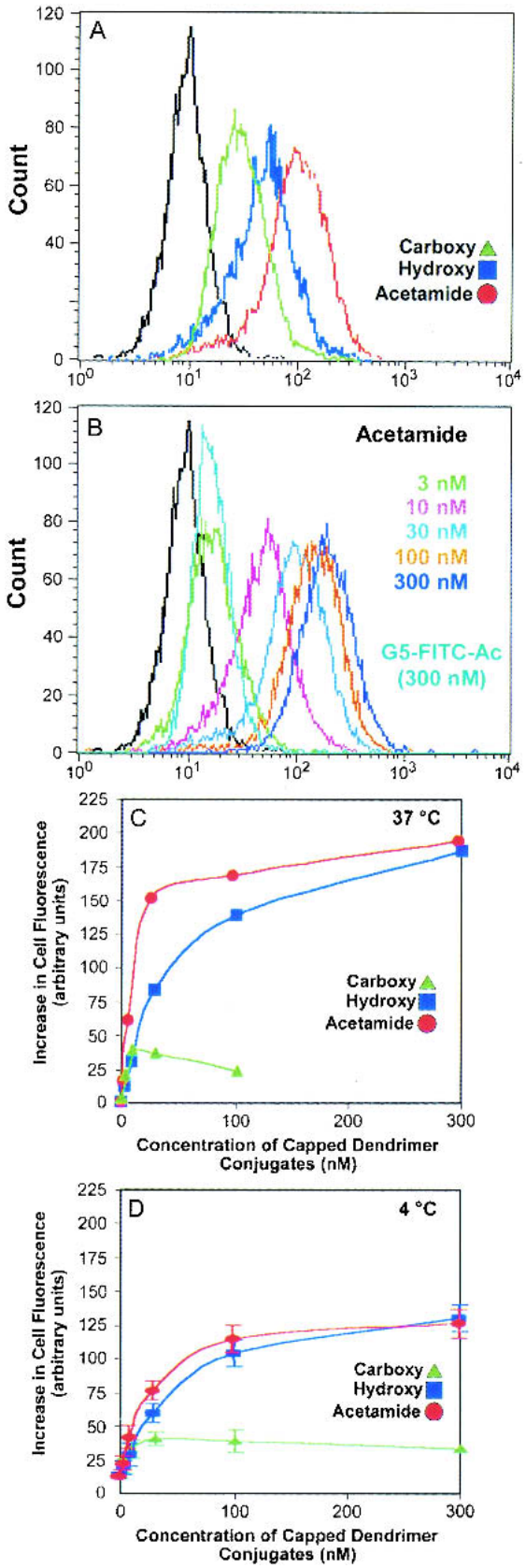

opment of multifunctional nanoscale devices is complex and requires active design and testing.

Our results clearly address a number of these issues and offer solutions. The covalent attachment of FA, averaging 2 to 3 molecules per dendrimer produced remarkable capability to target and internalize nanodevices in cells expressing the folate receptor. Efficient and specific targeting was achieved only when the primary amines on the surface of the dendrimer were covalently modified to prevent nonspecific, charge-based interactions. We were able to define concentrations of FA and FITC that when coupled to the polymer yielded functional and soluble material. For example, the conjugation of FITC to the polymer permitted the detection of cell binding and uptake using flow cytometry or confocal microscopy, but the product was only soluable when less than 20% of the amine groups were substituted with FITC. Using defined dendritic polymers of uniform molecular weight allowed us to design and manufacture a consistently soluble product within these limitations.

Although the affinity of monomeric FA for the folate receptor is very high with a Kd of at least 1 nM (19,20), the concentration required for half the maximal binding of folate conjugated macromolecules has been reported to be substantially higher suggesting lower affinity. For example, ^{125}I-BSA-folate conjugate has an apparent affinity of 10 nM (2), despite having no bulky aromatic groups present in the compound (as are present in flurochrome dyes). The techniques used in our study do not permit a precise calculation of the effective affinity and avidity of the nanodevices for the folate receptor. Nevertheless, it appeared that an approximately 23 nM concentration of the acetamide nanodevice and 53 nM concentration of the hydroxyl nanodevice was required to reach 50% of maximal binding. In competition experiments performed at 0°C, the concentration of free FA that reduced by 50% the amount of association reached by 30 nM of both dendrimer-folate conjugates was 25 to 30 nM; similar to the concentration required to compete free FA. This indicates that the binding of the optimized nanodevice is very efficient. The difference between the cell-associated nanodevice at 0°C and at 37°C documents that a significant degree of internalization of the conjugates occurs before the end of the 30 min incubation period. The acid-resistant binding of the nanodevice we observed might be due to this type of internalization. Since it was observed at 0°C, it is also possible that acid resistance is the result of multiple folate-receptor interactions stabilizing the binding of the nanodevice to the cell. This hypothesis remains unresolved because the unique characteristics and architecture of the dendrimers make it difficult to determine the interaction between the polymer-bound FA and folate receptors on cells. Further evaluation using techniques, such

Fig. 2. Binding of fluorescent dendrimer-folate conjugates to KB cells after 30 min incubation. All the experiments were performed at 37°C except Fig. 2d, which was at 4°C. Fig. 2a: cell-associated fluorescence increases with 30 nM of acetamide, hydroxyl, or carboxyl-surfaced dendrimer-folate conjugates. Fig. 2b: cell-associated fluorescence increases with increasing concentrations of acetamide-capped G5-FITC-FA. Significant background fluorescence was not observed until the concentration of the nontargeted control complex reached 300 nM. Fig. 2c and Fig. 2d cell-associated fluorescence as a function of dendrimer-folate concentration is presented for each of the three types of dendrimer, at 37°C in Fig. 2c and at 4°C in Fig. 2d. Amine-surfaced dendrimer-folate conjugates did not show binding at 30 min (data not shown).

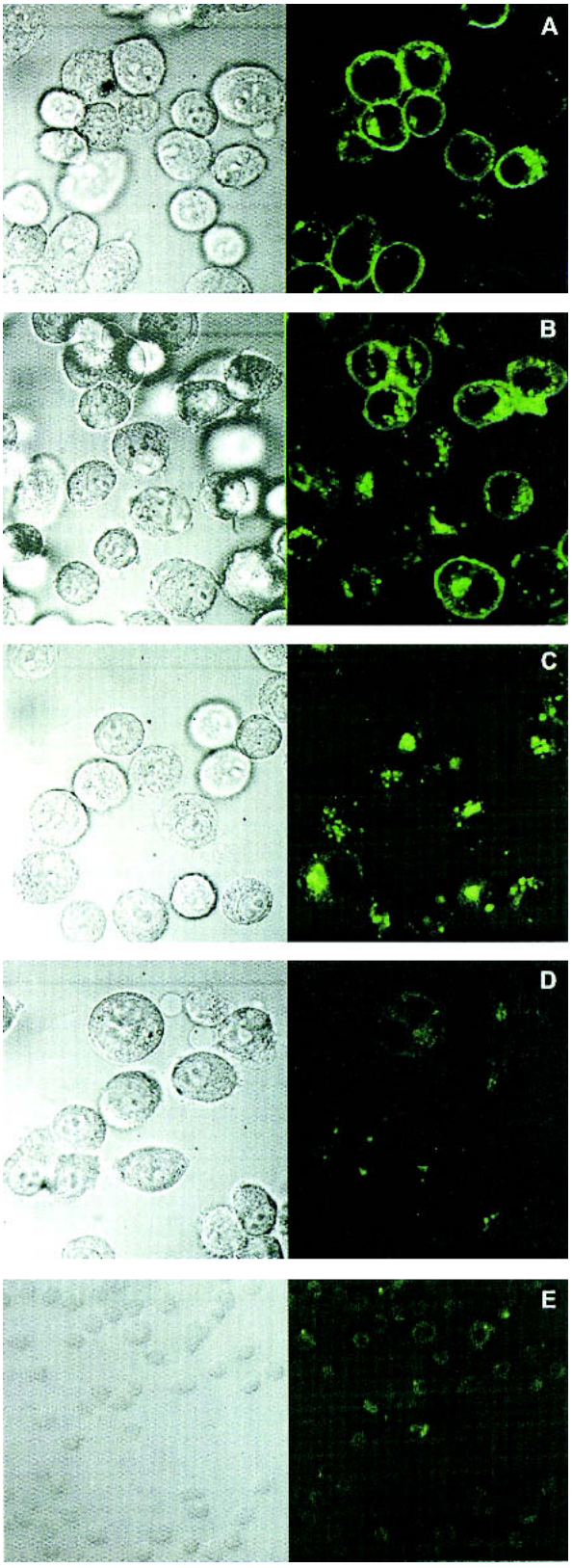

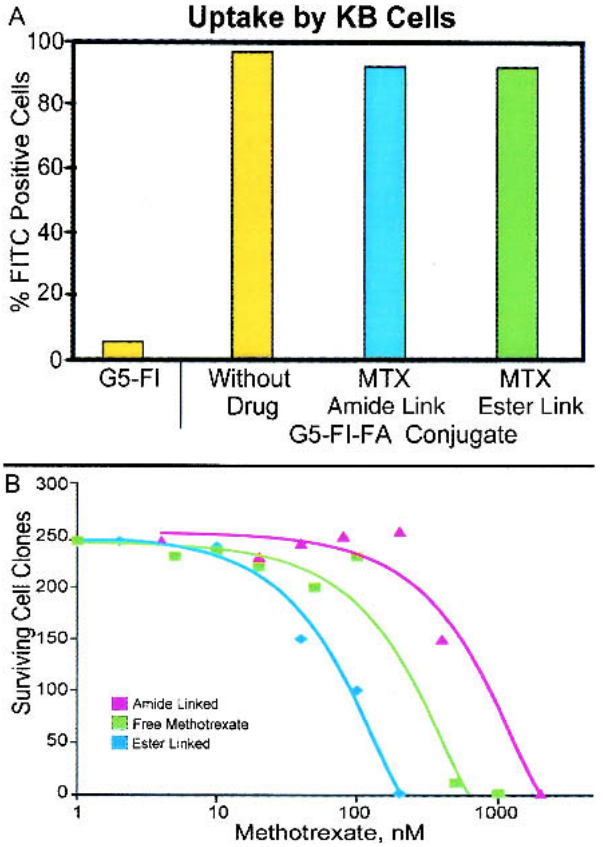

Fig. 4. Studies examining intracellular drug delivery with nanodevice. Flow cytometry data Fig. 4a show that the devices are readily taken into cells regardless of drug conjugate. A comparison of the efficiency in killing tumor cells Fig.4b of ester or ester conjugated drug and free methotrexate. The dendrimer- delivered drug is many times more efficient at killing the KB cells than methotrexate alone.

as atomic force microscopy, may better define the exact binding affinity of these devices.

It is significant that the structural predictions of the molecular modeling were confirmed by the experimental data obtained in KB cells. The higher probability for receptor interaction predicted for FA on the acetamide vs. the hydroxyl-modified dendrimer is confirmed by the lower concentration of acetimide-surfaced material required for 50% of the maximum association and by the relatively greater binding of the acetamide vs. the hydroxyl and carboxyl conjugates at equimolar concentrations. Examinations of a range of designs for nanodevices guided by molecular modeling has the potential to rapidly improve performance characteristics.

The tendency of the carboxyl conjugate to aggregate might explain the limited cell fluorescence observed reaching a plateau at four-fold over baseline, at concentrations above 30 nM (Fig. 2c and 2d). It is possible that aggregation of higher concentrations of the polymer prevented further binding to and uptake into the cells. This is especially important

Fig. 3. Confocal and fluorescence microscopic images of cells treated with acetamide-G5-FITC-FA. Each panel shows corresponding light (left) and fluorescent (right) images of the same slide. The top four show KB cells, and the bottom one shows NIH 3T3 cells that do not express the folate receptor. The upper three panels demonstrate the binding and uptake of folic acid dendrimer conjugates at 30 min, Fig. 3a; 6 h, Fig. 3b; and 24 h, Fig. 3c. As a control KB cells were incubated with fluorescent acetamide-G5-FITC not conjugated to folic acid Fig. 3d. The top three panels clearly demonstrate the binding and internalization of the nanodevice over 24 h.

given the much greater increases in cell-associated material observed with higher concentrations of the acetamide and hydroxyl-surfaced nanodevices, which provide functional advantages for these molecules.

Intracellular drug delivery has advantages over simple diffusion of drug into cells. Our drug internalizing devices were four-fold more efficient at inducing cytotoxicity in KB cells than free drug. This did not appear to be the result of polymer-related cytotoxicity, as the polymer controls were not cytotoxic. It is possible that releasing the drug within the cell will target it to the organelle where it is active. Since methotrexate directly competes with folic acid, delivering it through these receptors may be especially useful in this regard. Another possibility is that this type of delivery may overcome the effect of the multidrug resistance channel. The KB cells used in this study have an active multidrug resistance channel (21), so the cytotoxicity seen is especially significant. This type of channel is most efficient for drugs diffusing across the membrane and delivering drug deep within the cell may prevent it from being rapidly pumped out, and this possibility deserves further study.

This material has potential to target tumors *in vivo* because of its small size targeted by a high avidity multivalent ligand. It is likely that other delivery devices would not readily gain access to tumors from the vasculature due to their diameters between 40 to 100 nm, which is too big to transverse vascular pores (22) or a tendency to aggregate. This device is the same size as a small serum protein and therefore can pass through pores in the vasculature and infuse tumor cells directly (23). The rapid and specific binding and internalization of the device within tumor cells suggests the ability of this delivery system to transport biosensors, drugs, genetic material, and imaging agents into specific cells. Studies on this are warranted in appropriate animal models.

ACKNOWLEDGMENTS

This project has been funded in part with federal funds from the National Cancer Institute, National Institutes of Health under Contract No. NO1-CO-97111. We thank Douglas Swanson for his assistance in synthesizing the polymer used in these studies.

REFERENCES

1. A. C. Antony, M. A. Kane, R. M. Portillo, P. C. Elwood, and J. F. Kolhouse. Studies of the role of a particulate folate-binding protein in the uptake of 5-methyltetrahydrofolate by cultured human KB cells. *J. Biol. Chem.* **260**:14911–14917 (1985).
2. C. P. Leamon and P. S. Low. Delivery of macromolecules into living cells: a method that exploits folate receptor endocytosis. *Proc. Natl. Acad. Sci. USA* **88**:5572–5576 (1991).
3. J. J. Turek, C. P. Leamon, and P. S. Low. Endocytosis of folate-protein conjugates: ultrastructural localization in KB cells**.** *J. Cell Sci.* **106**:423–430 (1993).
4. I. G. Campbell, T. A. Jones, W. D. Foulkes, and J. Trowsdale. Folate-binding protein is a marker for ovarian cancer. *Cancer Res.* **51**:5329–5338 (1991).
5. S. D. Weitman, R. H. Lark, L. R. Coney, D. W. Fort, V. Frasca, V. R. Zurawski, Jr., and B.A Kamen. Distribution of the folate receptor GP38 in normal and malignant cell lines and tissues. *Cancer Res.* **52**:3396–3401 (1992).
6. J. F. Ross, P. K. Chaudhuri, and M. Ratnam. Differential regulation of folate receptor isoforms in normal and malignant tissues *in vivo* and in established cell lines. *Cancer* **73**:2432–2443 (1994).
7. R. J. Lee and P. S. Low. Folate-mediated tumor cell targeting of liposome-entrapped doxorubicin in vitro. *Biochim. Biophys. Acta* **1233**:134–144 (1995).
8. S. Wang, R. J. Lee, G. Cauchon, D. G. Gorenstein, and P. S. Low. Delivery of antisense oligodeoxyribonucleotides against the human epidermal growth factor receptor into cultured KB cells with liposomes conjugated to folate via polyethylene glycol. *Proc. Natl. Acad. Sci. USA* **92**:3318–3322 (1995).
9. C. P. Leamon and P. S. Low. Selective targeting of malignant cells with cytotoxin-folate conjugates. *J Drug Target.* **2**:101–112 (1994).
10. S. Wang, R. J. Lee, C. J. Mathias, M. A. Green, and P. S. Low. Synthesis, purification, and tumor cell uptake of ^{67g} ga-deferoxamine-folate, a potential radiopharmaceutical for tumor imaging**.** *Bioconjug. Chem.* **7**:56–62 (1996).
11. D. A. Tomalia, A. M. Naylor, and W. A. Goddard. Starburst dendrimers: molecular-level control of size, shape, surface chemistry, topology, and flexibility from atoms to macroscopic matter. *Angew. Chem. Int. Ed.* **29**:138–175 (1990).
12. A. Bielinska, J. F. Kukowska–Latallo, J. Johnson, D. A. Tomalia, and J. Baker, Jr. Regulation of in vitro gene expression using antisense oligonucleotides or antisense expression plasmids transfected using starburst PAMAM dendrimers. *Nucleic Acid Res.* **24**:2176–2182 (1996).
13. J. F. Kukowska–Latallo, A. Bielinska, J. Johnson, R. Spindler, D. A. Tomalia, and J. Baker, Jr. Efficient Transfer of genetic material into mammalian cells using starburst polyamidoamine dendrimers. *Proc. Natl. Acad. Sci. USA* **93**:4897–4902 (1996).
14. N. Malik and E. G. Evagorou, and R. Duncan. Dendrimer-platinate: a novel approach to cancer chemotherapy. *Anticancer Drugs* **10**:767–776 (1999).
15. E. C. Wiener, S. Konda, A. Shadron, M. Brechbiel, and O. Gansow. Targeting dendrimer-chelates to tumors and tumor cells expressing the high-affinity folate receptor. *Invest. Radiol.* **32**:748–754 (1997).
16. N. Malik, R. Wiwattanapatapee, R. Klopsch, K. Lorenz, H. Frey, J. W. Weener, E. W. Meijer, W. Paulus, and R. Duncan. Dendrimers: relationship between structure and biocompatibility in vitro, and preliminary studies on the biodistribution of ^{125}I-labelled polyamidoamine dendrimers *in vivo*. *J. Control. Release* **65**:133–148 (2000).
17. E. C. Wiener, S. Konda, A. Shadron, M. Brechbiel, and O. Gansow. Targeting dendrimer-chelates to tumors and tumor cells expressing the high-affinity folate receptor. *Invest. Radiol.* **32**:748–754 (1997).
18. D. A. Tomalia, H. Baker, J. Dewald, M. Hall, G. Kallos, S. Martin, J. Roeck, J. Ryder, and P. Smith. A new class of polymers - starburst-dendritic macromolecules. *Polymer J.* **17**:117–132 (1985).
19. B. A. Kamen and J. D. Caston. Properties of a folate binding protein (FBP) isolated from porcine kidney. *Biochem. Pharmacol.* **14**:2323–2329 (1986).
20. P. C. Elwood, M. A. Kane, R. M. Portillo, and J. F. Kolhouse. The isolation, characterization, and comparison of the membrane- associated and soluble folate-binding proteins from human KB cells. *J. Biol. Chem.* **261**:15416–15423 (1986).
21. A. S. Bauchez, J. Lunardi, C. Pernin, D. Marti-Battle, and D. Fagret. Detection of chemoresistance profile of cell lines K562, KB, GLC4, and HL60 through characterisation of the hmdr1, mrp, and Irp transcripts. *In Vivo* **15**:101–104 (2001).
22. G. Kong, R. D. Braun, and M. W. Dewhirst. Hyperthermia enables tumor-specific nanoparticle delivery: effect of particle size. *Cancer Res.* **60**:4440–4445 (2001).
23. J. F. Ross, P. K. Chaudhuri, and M. Ratnam. Differential regulation of folate receptor isoforms in normal and malignant tissues *in vivo* and in Established cell lines. *Cancer* **73**:2432–2443 (1994).